Membrane electrolysis for recovering Sb and Bi from elution solutions of ion-exchange resins used in copper electrorefining: a cyclic voltammetric study

Kayo Santana Barros [1,2,3*]; André Luiz Vargas Machado [1];
Vicente Schaeffer Vielmo [1]; Svetlozar Velizarov [3]; Jane Zoppas Ferreira [1];
Valentín Pérez-Herranz [2]; Andréa Moura Bernardes [1]

[1] Post-Graduation Program in Mining, Metallurgical and Materials Engineering (PPGE3M), Federal University of Rio Grande do Sul (UFRGS), Av. Bento Gonçalves, 9500, 91501-970, Porto Alegre, Brazil.

[2] IEC Group, ISIRYM, Universitat Politècnica de València – Spain. Address: Camí de Vera s/n, 46022, P.O. Box 22012, València E-46071, Spain

[3] Associated Laboratory for Green Chemistry-Clean Technologies and Processes (LAQV), REQUIMTE, Chemistry Department, FCT NOVA, Universidade Nova de Lisboa, Caparica 2829-516, Portugal

[*]Corresponding author: kayo.barros@fct.unl.pt

Abstract: Antimony (Sb) and bismuth (Bi), which have been considered critical raw materials by the European Commission, cause inconveniences to copper production when they are present as impurities in copper electrorefining solutions. Therefore, ion-exchange resins to extract Sb and Bi from copper-containing electrolytes have typically been applied; after the adsorption of the metals, the elution step is conducted with an HCl solution to desorb them. In the present study, a novel membrane electrolysis system with a cation-exchange membrane was proposed to extract Sb and Bi ions from the elution solution, and a cyclic voltammetric study was carried out to evaluate the influence of the most important operating parameters on the process performance, such as Sb, Bi and HCl concentration, dilution factor of the solution, the presence of thiourea as a complexing agent, the presence of iron as an impurity, and temperature. The obtained voltammograms indicated that the simultaneous presence of the metals in solution alters considerably their electrodeposition and oxidation pattern when compared to the solutions with pure metals. The reactions of electrodeposition of both metals are not electrochemically reversible and the diffusion control for bismuth is greater than that for antimony. The increase in the concentration of Sb affects its electrodeposition kinetically, whereas that of Bi is affected both kinetically and thermodynamically. The increase in HCl concentration disfavors the electrodeposition of both metals. Diluting the solution reduces the energy consumption and prolongs the membrane lifespan. Increasing the temperature reduces the cathodic potential to deposit the metals but favors the hydrogen evolution reaction. The presence of iron as an impurity does not affect the electrodeposition of both metals, whereas the use of thiourea as a complexing agent must be avoided because it impairs their electrodeposition.

Keywords: electrodeposition; cyclic voltammetry; antimony; bismuth; thiourea.

1. Introduction

Technological development is highly dependent on copper due to its important properties, such as high electrical and thermal conductivities, as well as ductility, which make it a very versatile material [1]. Copper can be obtained in nature from oxide and sulfide ores, and the ore type determines the process steps it must undergo, as several purification steps need to be conducted for eliminating impurities and obtaining a high-purity copper product. In general, sulfide ores are subjected to the following treatment stages: comminution, mineral concentration via flotation, pyrometallurgical route (smelting and converting) and electrorefining. A detailed description of copper production from sulfide minerals can be found in our recent review [2].

In the electrorefining step, copper is purified via electrolysis by introducing copper anodes into a cell containing an electrolyte composed of sulfuric acid, copper sulfate and some additives which improve the quality of the deposit, such as thiourea, bone glue, and chloride ions [3]. As electric current is applied, metallic copper at the anode oxidize and migrate from the anode towards the cathode, which is the high-purity copper product. At the end of electrolysis, some impurities remain at the anode, being called anode scrap. Other impurities dissolve along with copper and form an insoluble material referred to as anode slime, which is deposited at the bottom of the cell. There are also impurities that are released along with copper but remain dissolved in the electrolyte, thus contaminating it and hindering copper purification. Among the major impurities that affect copper electrorefining, Sb and Bi ions are the most critical ones because their standard reduction potentials are similar to that of copper [4], which may lead to cathode contamination, anode passivation, while also increasing anode slime production. In this sense, some techniques are generally used to treat the contaminated copper electrolyte. One of the main methods used is forwarding part of the electrolyte to an electrowinning cell. However, this method involves high energy consumption and risks to human health due to the formation of the toxic arsine gas [5]. Another method often used is to add arsenic into the electrolyte so that the solubility of antimony and bismuth is reduced, leading to the deposition of the metals as part of the anode slime. This technique also presents some disadvantages, such as the use of additional reagents, the risks associated with the arsenic toxicity and the loss of Sb and Bi in the slime [5,6].

Antimony and bismuth have been considered critical raw materials by the European Commission, indicating that both metals present high risk of depletion if their obtaining

methods are not reevaluated [7,8]. The major limitations faced in obtaining these metals in the coming years will be an intense reduction in the content of ores, difficulties in exploring remote regions, and high energy costs [7,9]. The main application of Sb is for flame-retardants, but it is also used in the production of lead-acid batteries, in the electronic industry, in pigments, pesticides, medicines, and detonators. Some of the main applications of Bi are the same as those of Sb, in addition to being applied in cosmetics and in the pharmaceutical industry [8,10–12]. Bi-Sb alloys are also valuable materials with good solderability and high corrosion resistance, being often used as semiconductors in electronics [13–16].

Considering the importance of obtaining Sb and Bi from secondary resources in mining processes, several authors have tried to extract them from the copper electrorefining solution using alternative methods to the conventional ones, such as chemical precipitation [17,18], activated carbon [19,20], solvent extraction [21,22], chemical leaching [23], electrowinning [7], electrodialysis [24], and ion-exchange resins [6,25]. The use of ion-exchange resins for this purpose stands out since they have been intensively tested in the literature [2], besides being already used industrially worldwide. The main parameters evaluated in these studies are the mass of resins, contact time, Sb and Bi concentrations, temperature, and use of additives. In addition, authors have evaluated the effect of antimony oxidation from Sb(III) to Sb(V) on the ion-exchange process, the undesirable precipitation of metals in the resins, and the presence of ferric ions as an impurity [6,25–30].

After treating the contaminated copper electrolyte by ion-exchange resins, which are usually aminophosphonic, it is necessary to carry out the elution step of the adsorbed metals. Elution is usually conducted with HCl solutions at a concentration of 5-7 mol/L in order to promote ion exchange between protons and the adsorbed metals. In this case, Sb and Bi ions are eluted as complex chloride-based anions [6]. Several studies have been carried out on the elution stage, mainly to evaluate the influence of resin poisoning by Sb(V) and the use of thiourea as a complexing agent [6,26,31,32].

The elution solution loaded with Sb(III) and Bi(III) ions is usually treated by fractional distillation in order to recover HCl. This method presents disadvantages such as the generation of toxic and corrosive Cl_2, while also hindering the recovery of the pure metals. To the best of our knowledge, there are no critical studies reported in the open literature on alternative methods to fractional distillation for treating the elution solution

from ion-exchange resins used in copper electrorefining. Cifuentes et al. [4] carried out a study on the use of electro-electrodialysis as an alternative method, but the Sb and Bi ions were not present in the HCl solutions. Electro-electrodialysis allows for the separation of ionic species through membranes selective for anions or cations, while specific reactions occur at the electrodes during the electrodeposition of the species [33,34]. This system, which is composed of at least two membranes and three compartments, generates a diluted solution in one of the compartments and more concentrated solutions in the other compartments [35,36]. Although electro-electrodialysis is very versatile, the extremely higher concentration of protons compared to Sb and Bi ions can make its use unfeasible to treat elution solutions. To overcome this limitation, other techniques should be evaluated, and a possible alternative is membrane electrolysis.

Membrane electrolysis is a process in which the same principles as electro-electrodialysis are exploited, but the former is composed of only two compartments separated by a cation- or anion-exchange membrane, making it considerably simpler than the latter [35]. In membrane electrolysis systems, the desired species are concentrated in one of the compartments, while the other species are retained in the other compartment. Thus, its efficiency depends strongly on the ionic species present in the electrolyte and the operating conditions, such as ion concentration, pH, and temperature [37]. Therefore, cyclic voltammetric studies are essential to guarantee the efficiency of membrane electrolysis by evaluating the electrodeposition kinetics of the species and determining the optimal operating conditions. The use of membrane electrolysis for treating the elution solution of ion-exchange resins used in the treatment of copper electrorefining solutions may be very promising, as it is an environment-friendly technique which does not generate waste, allows the extraction and recovery of valuable metals, such as Sb and Bi, and the return of pure HCl to the elution step. However, studies must be carried out to make this method technically and economically viable.

The present work aimed to evaluate, by cyclic voltammetry, the influence of the most important operating parameters on the electrodeposition of Sb and Bi present in HCl solution in order to foster membrane electrolysis applications. The experiments were carried out with synthetic solutions simulating the one generated in the elution step of ion-exchange resins used to treat copper electrorefining solutions contaminated with those metals. The parameters evaluated were Sb(III), Bi(III) and HCl concentration, dilution factor of the solution, the presence of thiourea as a complexing agent, the

presence of iron ions as an impurity, and temperature. The electrodeposition kinetics of the species were also studied by evaluating the effects of the scan rate on the cyclic voltammograms.

2. Materials and Methods

2.1. Membrane electrolysis cell

The experiments were conducted in a two-compartment cell separated by a commercial cation-exchange membrane. The anode compartment was fed with 100 ml of a H_2SO_4 solution, whereas the cathode compartment was fed with 100 ml of the working solution composed of HCl, Sb(III) and Bi(III) ions. The solutions were prepared with H_2SO_4, HCl (Química Moderna Ind. e Com. Ltda, Barueri, Brazil), Sb_2O_3, BiO_3 (Dinâmica Química Contemporânea, Indaiatuba, Brazil), and distilled water. A potentiostat/galvanostat (Autolab PGSTAT 20, Utrecht, The Netherlands) was used for controlling the experiments. The tests were performed within the potential range of −1.3 V to 1.5 V. All the experiments were conducted in triplicate and the estimated relative error between the curves was below 5%. A schematic representation of the cell is presented in Figure 1. This cell configuration was used because antimony and bismuth in highly concentrated HCl solutions form mainly complex chloride-based anions [6,7]. The cation-exchange membrane avoids the migration of these anions, as well as the transport of Cl^- ions, towards the anode. Thus, the metals are deposited at the cathode without formation of gaseous Cl_2 at the electrodes, which is corrosive and harmful to human health.

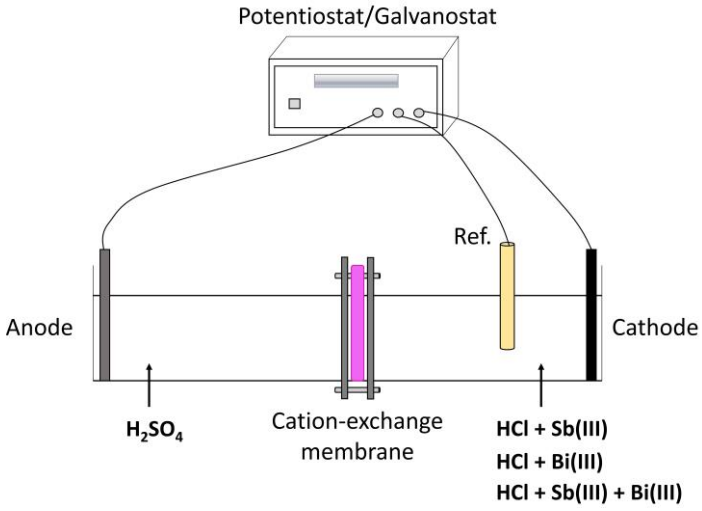

Figure 1 – A schematic representation of the membrane electrolysis cell.

The working, reference and counter electrodes were made of titanium, Ag/AgCl and platinum, respectively. In the evaluation of the temperature effect, titanium was used as working electrode, platinum as reference electrode, and titanium coated with titanium and ruthenium oxides ($70RuO_2/30TiO_2$) as counter electrode due to the low stability of Ag/AgCl at high temperatures. Before each experiment, the working and counter electrodes were polished with 240 and 500 emery paper, rinsed with distilled water and dried.

2.2. Ion-exchange membrane

The cation-exchange membrane used was the IONSEP-HC-C, also known as HDX100 (Hangzhou Iontech Environmental Technology Co., Ltd., China), which is heterogeneous and contains sulfonic acid groups. This membrane has been widely used in electrodialytic processes [38,39] and its characteristics are described elsewhere [40].

2.3. Experimental conditions

The working solution present in the cathode compartment contained 1 g/L of Sb(III) ions, 0.1 g/L of Bi(III) ions and 6 mol/L of HCl, and its composition was based on the elution solution originating from ion-exchange resins used in the copper electrorefining process [2]. In the evaluation of the presence of thiourea as a complexing agent, the following molar ratios of thiourea/antimony were tested: 0; 0.5; 1.0; 2.0; 3.0. For the evaluation of the presence of ferric ions as an impurity, the Fe(III) concentration was set at 0.1 g/L, which was based on its concentration in the copper electrolyte reported by Cifuentes et al. [41].

Except for the temperature effect evaluation, the experiments were carried out at room temperature (~20ºC). In the temperature evaluation experiments, four working temperatures were tested: 20ºC, 30ºC, 40º and 50ºC; before each experiment, the cathodic and anodic solutions were heated and kept at 2ºC above the working temperature (22ºC, 32ºC, 42ºC, 52ºC) for 5 minutes in a beaker containing the electrodes. Then, the solutions and electrodes were transferred as quickly as possible to the membrane electrolysis cell for conducting the test; the temperature of both solutions in the cell was monitored and the experiments were started when the working temperature was reached (20ºC, 30ºC, 40ºC, 50ºC). The final temperature of the solutions was also measured, which was found

to be approximately 2°C below the working temperature (18ºC, 28ºC, 38ºC, 48ºC), respectively. Therefore, the temperatures reported herein varied by up to -2ºC due to their decrease throughout the experiments.

The solution in the anodic compartment was composed of H_2SO_4 containing the same molar concentration of protons as the one on the cathodic side. Thus, in most of the tests, the H_2SO_4 solution presented a concentration of 3 mol/L, except for the evaluations of the effects of solution dilution and of the HCl concentration in the cathodic solution. Table 1 presents the experimental conditions of the experiments performed.

Table 1 – Experimental conditions of the tests

Evaluation	Experimental conditions							
	Scan rate (V/s)	Sb(III) (g/L)	Bi(III) (g/L)	HCl (mol/L)	Thiourea (mol/L)	Fe(III) ions (g//L)	H_2SO_4 - anode (mol/L)	Temperature (ºC)
Presence of Sb(III) and Bi(III) ions	0.02	0; 1	0; 0.1	6	0	0	3	~20
Scan rate	0.005; 0.01; 0.02; 0.04; 0.06; 0.08; 0.1	0; 1	0; 0.1	6	0	0	3	~20
Sb(III) and Bi(III) concentration	0.02	0; 0.25; 0.5; 0.75; 1; 1.5; 2; 4	0; 0.025; 0.05; 0.075; 0.1; 0.15; 0.2; 0.4	6	0	0	3	~20
HCl concentration	0.02	0; 1	0; 0.1	4; 5; 6; 7	0	0	2; 2.5; 3; 3.5	~20
Dilution factor	0.02	0; 0.35; 0.5; 0.75; 1 (0%, 35%, 50%, 75% and 100% of the original solution, respectively)	0; 0.035; 0.05; 0.075; 0.1 (0%, 35%, 50%, 75% and 100% of the original solution, respectively)	2.1; 3.0; 4.5; 6 (35%, 50%, 75% and 100% of the original solution, respectively)	0	0	1.05; 1.5; 2.25; 3 (35%, 50%, 75% and 100% of the original solution, respectively)	~20
Temperature	0.02	0; 1	0; 0.1	6	0	0	3	20; 30; 40; 50
Presence of thiourea	0.02	0; 1	0; 0.1	6	0; 0.0041; 0.0082; 0.016; 0.025 (Thiourea/Sb molar ratio of 0; 0.5; 1; 2 and 3, respectively)	0	3	~20
Presence of Fe(III) ions	0.02	0; 1	0; 0.1	6	0	0.1	3	~20

3. Results and Discussion

3.1. Effect of the presence of Sb and Bi in HCl solution

Speciation diagrams for the solutions of Sb (1 g/L) + HCl (6 mol/L), Bi (0.1 g/L) + HCl (6 mol/L), and Sb (1 g/L) + Bi (0.1 g/L) + HCl (6 mol/L) were constructed with the aid of Hydra-Medusa software [42] using equilibrium constants data present in ref. [14]. According to Figure 2, antimony and bismuth are present in the working solution (at pH 0) mainly as $SbCl_6^{3-}$, $SbCl_5^{2-}$ and $BiCl_6^{3-}$, $BiCl_5^{2-}$ species, respectively. Solutions containing Sb also present a relevant concentration of $SbCl_4^-$ species, whereas the concentration of $BiCl_4^-$ can be considered negligible in the solutions containing Bi.

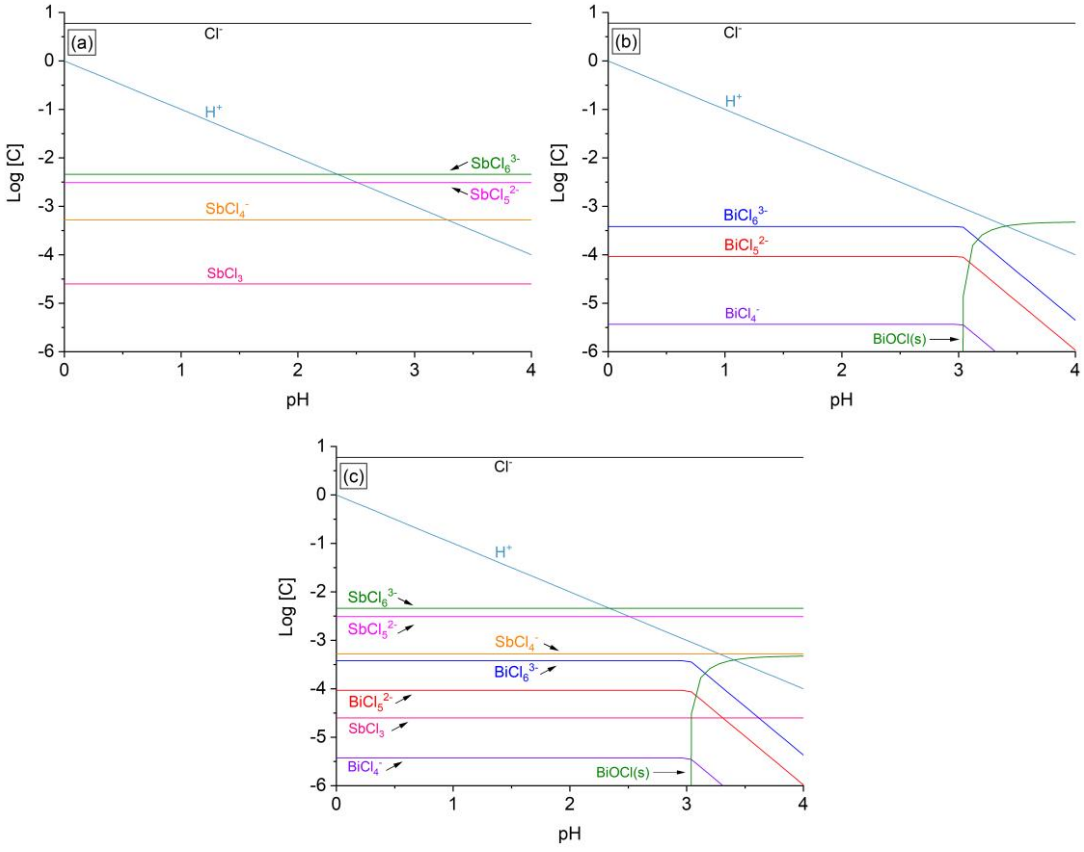

Figure 2 – Speciation diagram constructed for the solution of (a) Sb (1 g/L)+HCl (6 M), (b) Bi (0.1 g/L)+HCl (6 M), and (c) Sb (1 g/L)+Bi (0.1 g/L)+HCl (6 M).

Figure 3 presents the cyclic voltammograms constructed with Sb+HCl, Bi+HCl and Sb+Bi+HCl solutions at 0.02 V/s. Typical cyclic voltammetry curves were obtained for

antimony and bismuth in HCl solution, indicating that both metals can be deposited onto the Ti substrate.

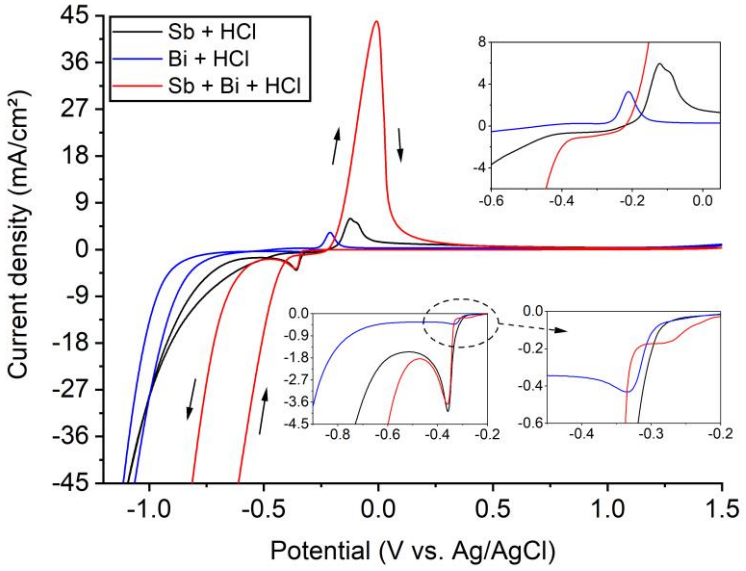

Figure 3 - Cyclic voltammograms constructed at a scan rate of 0.02 V/s with solutions of Sb (1 g/L)+HCl (6 M), Bi (0.1 g/L)+HCl (6 M), Sb (1 g/L)+Bi (0.1 g/L)+HCl (6 M). Insets show the oxidation and reduction peaks.

When Sb and Bi are present separately in the HCl solution (Sb+HCl and Bi+HCl), only one reduction peak is observed, which is related to the deposition of the elemental metal from Sb(III) and Bi(III) species, respectively. The Sb and Bi reduction peaks show a significant difference in their current density values (-4.0 mA/cm² and -0.43 mA/cm², respectively) mainly due to the higher Sb concentration. Regarding the overpotential, both metals begin to deposit at approximately -0.28V, with the Sb peak appearing at -0.36V and the Bi peak at -0.33V. The reduction peaks of each metal present distinct shapes. Note that the Sb peak is sharp and well defined, whereas the Bi peak is smoother and extends towards more negative overpotentials, showing a limiting current density. This may be an indication of the greater diffusion control for bismuth deposition than for that of antimony [43]. The considerably lower concentration of Bi may also have favored this behavior. The shape of the curves obtained agrees well with the cyclic voltammetric curves reported by Kang et al. [44], which were obtained with concentrations of Sb (1.2 g/L) and Bi (0.2 g/L) similar to those tested in our work, but at a much lower concentration of HCl (0.35 mol/L).

When Sb and Bi are present simultaneously in the solution (Sb+Bi+HCl), the deposition of the metals takes place in two steps. Firstly (at -0.2V), there is a gradual negative shift of current density towards more negative potentials, showing a plateau related to the deposition of Bi. Then, from approximately -0.32V, the cathodic current density shows a strong increase reaching a peak at -0.36V, which is related to the deposition of Sb. Note that the peaks of Sb when it is present separately and together with Bi in the solution are practically superimposed, which indicates that the presence of Bi practically does not affect the current density and potential values at which Sb is electrodeposited. This can be explained by the complexes formed in each of the solutions evaluated (Figure 2). Note that the predominant species in solutions where Sb and Bi are present separately and simultaneously are the same ($SbCl_6^{3-}$, $SbCl_5^{2-}$, $BiCl_6^{3-}$, $BiCl_5^{2-}$) and there is no formation of complexes involving both metals. Thus, the metals are electrodeposited independently.

For potential values more negative than approximately -0.5V (Sb+Bi+HCl), -0.6V (Sb+HCl) and -0.7V (Bi+HCl), the cathodic current density shows a strong increase towards negative values due to the hydrogen evolution reaction (HER). Note that the behavior caused by this reaction is quite different for each solution evaluated. When Sb and Bi are present simultaneously in the solution, HER occurs at considerably lower cathodic potentials than when the metals are individually present. Therefore, the simultaneous deposition of the metals is hindered, since HER tends to reduce the current efficiency and, thus, the quality of the deposit. When the electrodeposition occurs under intense HER, nonadherent powder deposits are generally obtained [15,45].

When the potential scan is reversed, anodic peaks are observed due to the dissolution of metals into the solution. For the Bi+HCl solution, a single and well-defined peak is observed, as to be expected, due to the oxidation of Bi to Bi(III). For the Sb+HCl solution, the peak shows a subtle post-wave: the main peak is due to the oxidation of Sb to Sb(III), whereas the post-wave may have appeared due to the presence of an antimony oxide. When both metals are present simultaneously in the solution, a single anodic peak is obtained, indicating that Sb and Bi are not oxidatively dissolved independently of one another. This agrees with the results obtained by Besse et al. [15], who evaluated the morphology of Sb-Bi films electrodeposited in NaCl 4 mol/L and HCl 1 mol/L media.

Upon the reverse scan, a single current crossover is observed for the solution of Bi+HCl at all scan rates. On the other hand, two current crossovers appear for the solutions of Sb+HCl and Sb+Bi+HCl, which is a typical behavior for deposition processes involving

nucleation, indicating that stable growth centers are formed at the substrate surface when antimony is present [46,47]. For the solution of Sb+HCl at a scan rate of 0.02 V/s, the potential of the higher cathodic current crossover is -0.32V (nucleation potential), whereas the other cathodic current crossover is -0.25V (crossover potential). For the solution of Sb+Bi+HCl at a scan rate of 0.02 V/s, the nucleation potential is -0.34V, whereas the crossover potential is -0.23V.

It can be inferred that the presence of the metals together in the Sb+Bi+HCl solution caused a significant increase in the current density of the oxidation peak, in addition to a shift towards more positive potentials. After the oxidation peak of Sb and Bi, when they are together or individually present in the solution, the current density remains at zero as the potential increases positively, indicating the complete oxidative dissolution of the metals at the electrode surface [48].

3.2. Scan rate evaluation

Figure 4 shows the cyclic voltammetry curves constructed for the (a) Sb+HCl, (b) Bi+HCl, and (c) Sb+Bi+HCl solutions at scan rates between 0.005 V/s – 0.1 V/s. The values of current density and potential of the cathodic (i_c, E_c) and anodic (i_a, E_a) peaks of the metals in each of the solutions tested were obtained from Figure 4, and the results are shown in Table 2. The values of cathodic (Q_c) and anodic (Q_a) charges are also shown in Table 2, which were determined by integration of the area under the cathodic and anodic peaks, respectively, of the current vs. time curves. The Table also presents the current density ratios of the anodic and cathodic peaks ($|i_a/i_c|$), the difference between the potential of both peaks ($E_a - E_c$), and the charge ratios of the anodic and cathodic peaks (Q_a/Q_c) obtained at each scan rate.

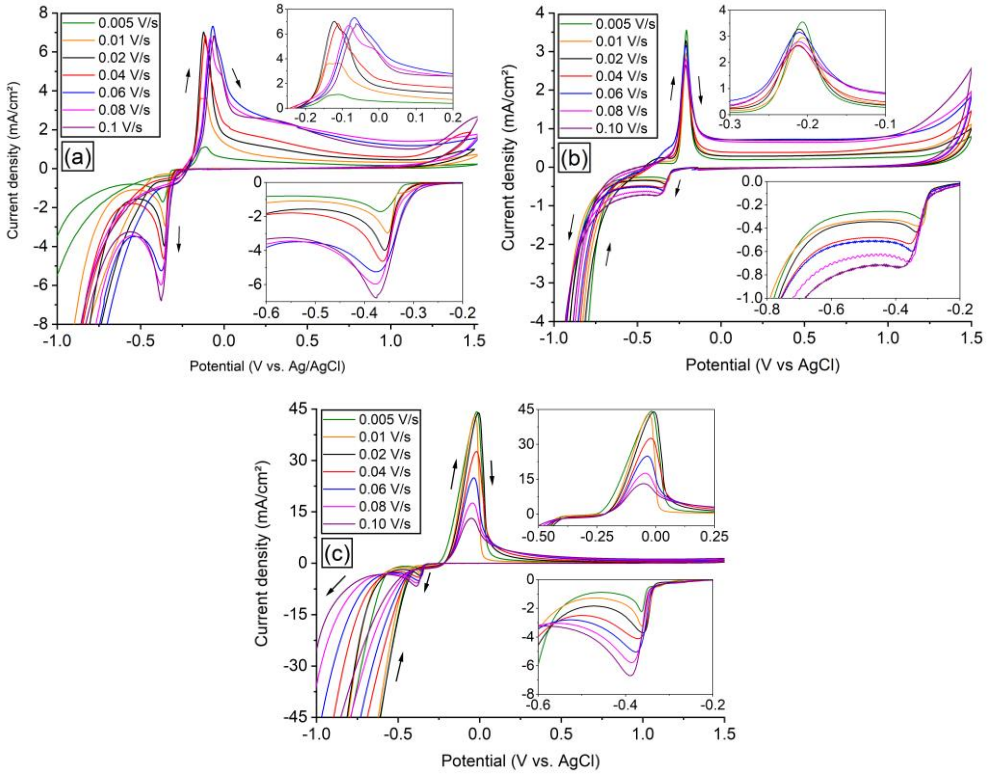

Figure 4 – Cyclic voltammograms for solutions of (a) Sb+HCl, (b) Bi+HCl and (c) Sb+Bi+HCl at different scan rates (0.005 – 0.10 V/s). Insets show the oxidation and reduction peaks.

Table 2 - Values of current density, potential and charge of the cathodic (i_c, E_c, Q_c) and anodic (i_a, E_a, Q_a) peaks of the metals in each of the solutions shown in Figure 4.

Solution: Sb + HCl									
	Anodic peak			Cathodic peak					
Scan rate (V/s)	$i_a\ (mA/cm^2)$	$E_a\ (V)$	$Q_a\ (C/cm^2)$	$i_c(mA/cm^2)$	$E_c(V)$	$Q_c\ (C/cm^2)$	$\lvert i_a/i_c\rvert$	$E_a - E_c\ (V)$	Q_a/Q_c
0.005	1.1	-0.14	0.043	-1.69	-0.37	0.057	0.7	0.23	0.8
0.010	2.6	-0.14	0.057	-2.99	-0.36	0.037	0.9	0.23	1.5
0.020	6.6	-0.13	0.038	-3.98	-0.36	0.025	1.3	0.23	1.5
0.040	4.1	-0.12	0.020	-4.38	-0.38	0.017	0.9	0.26	1.2
0.060	5.9	-0.10	0.021	-5.01	-0.39	0.018	1.2	0.26	1.2
0.080	5.8	-0.10	0.013	-5.94	-0.39	0.014	1.0	0.29	0.9
0.100	4.1	-0.11	0.010	-6.31	-0.41	0.012	0.6	0.30	0.8
Solution: Bi + HCl									
	Anodic peak			Cathodic peak					
Scan rate (V/s)	$i_a(mA/cm^2)$	$E_a\ (V)$	$Q_a\ (C/cm^2)$	$i_c(mA/cm^2)$	$E_c(V)$	$Q_c\ (C/cm^2)$	$\lvert i_a/i_c\rvert$	$E_a - E_c$ (V)	Q_a/Q_c
0.005	2.6	-0.20	0.020	-0.3	-0.32	0.006	7.8	0.12	3.5
0.010	2.9	-0.21	0.012	-0.4	-0.32	0.004	7.8	0.12	2.7
0.020	3.2	-0.21	0.011	-0.4	-0.33	0.004	7.7	0.12	2.6
0.040	2.6	-0.21	0.007	-0.5	-0.36	0.003	4.9	0.15	2.2
0.060	3.1	-0.21	0.005	-0.6	-0.35	0.002	5.1	0.14	3.0
0.080	2.8	-0.21	0.004	-0.7	-0.36	0.002	4.1	0.16	2.4
0.100	2.6	-0.21	0.003	-0.7	-0.38	0.001	3.6	0.17	2.4
Solution: Sb + Bi + HCl									
	Anodic peak			Cathodic peak					
Scan rate (V/s)	$i_a(mA/cm^2)$	$E_a\ (V)$	$Q_a\ (C/cm^2)$	$i_c(mA/cm^2)$	$E_c(V)$	$Q_c\ (C/cm^2)$	$\lvert i_a/i_c\rvert$	$E_a - E_c$ (V)	Q_a/Q_c
0.005	44.1	-0.01	1.313	-2.2	-0.37	0.041	20.5	0.35	32.2
0.010	46.1	-0.01	0.540	-3.0	-0.36	0.032	14.7	0.35	16.7
0.020	44.0	-0.01	0.314	-3.7	-0.36	0.022	11.8	0.35	14.5
0.040	32.0	-0.02	0.127	-4.1	-0.37	0.017	7.8	0.35	7.6
0.060	25.0	-0.03	0.067	-5.0	-0.38	0.014	5.0	0.34	4.9
0.080	18.0	-0.04	0.040	-5.8	-0.38	0.014	3.1	0.35	2.9
0.100	13.0	-0.05	0.029	-6.7	-0.39	0.012	1.9	0.34	2.5

In the forward scan, an increase in scan rate shifted the reduction peaks towards more negative current densities. This was expected since the thickness of the diffusion boundary layer is reduced at faster scan rates, which increases the current density [49]. Figure 5 shows the plot of current density of the cathodic peaks (i_c) versus the square root of the scan rate ($v^{0,5}$) based on the Randles−Sevcik equation (Equation 1). In Equation 1, n is the number of electrons transferred in the reduction step, D_0 and C_0 are the diffusion coefficient and bulk concentration of the analyte, respectively, F is the Faraday constant, T is temperature and R is the universal gas constant [49,50]. The curves of i_c vs. $v^{0,5}$ showed different shapes for each solution: for Bi+HCl, it showed a linear behavior

($R^2 = 0.992$), whereas for the solutions with antimony (Sb+HCl and Sb+Bi+HCl) the curves showed a change in their behavior at 0.04 V/s [0.2 $(V/s)^{1/2}$].

$$i_c = 0.446nFC_0\left(\frac{nFvD_0}{RT}\right)^{1/2} \quad \text{Eq. (1)}$$

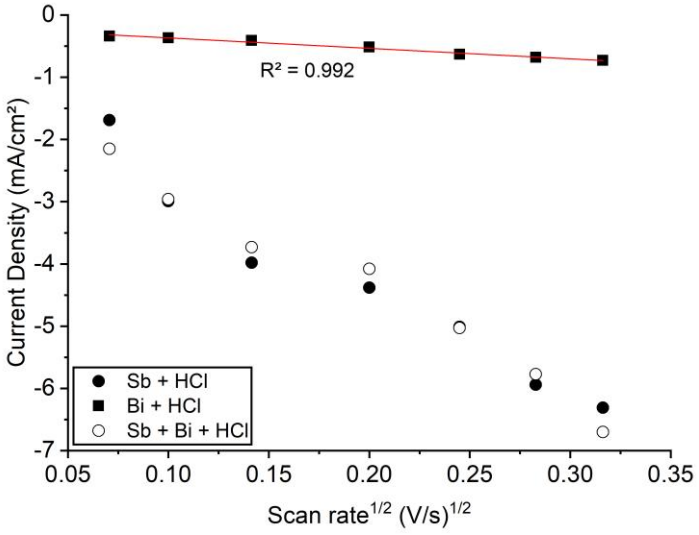

Figure 5 – Relation of the square root of scan rate and current density of the reduction peaks obtained with the solutions of Sb+HCl, Bi+HCl, and Sb+Bi+HCl, respectively.

In the reverse scan, an anomalous effect occurred on the oxidation peaks. For the Sb+HCl and Bi+HCl solutions, as the scan rate increased from 0.005 V/s to 0.02 V/s, the current density of the anodic peaks also increased. This behavior was expected since the relationship between current density (i) and scan rate (v) tends to be similar in the reduction and oxidation steps. However, at scan rates above 0.04 V/s, the current density of the anodic peak (i_a) remained practically unchanged, showing a subtle downward trend. This is more evident for the Sb+Bi+HCl solution, as i_a remained constant between 0.005 V/s – 0.02 V/s and showed a strong reduction between 0.04 V/s - 0.1 V/s. As the anodic peaks did not follow a linear behavior as a function of scan rate, the plot of $i_a$versus $v^{0,5}$ based on the Randles−Sevcik equation is not shown herein. This change in the behavior of the reduction and oxidation peaks of the curves at 0.04 V/s, especially for the Sb+Bi+HCl solution, indicates that this scan rate value delimits the scan rate range

within which the reactions exhibit more reversible or non-reversible behaviors, as will be discussed below.

According to Table 2, the i_a/i_c and Q_a/Q_c ratios deviate from unity mainly for the solutions containing bismuth (Bi+HCl and Sb+Bi+HCl). Non-unity i_a/i_c and Q_a/Q_c ratios are typical of irreversible processes and indicate homogeneous kinetic behavior or other complex phenomena occurring at the electrode. Note in Table 2 that the i_a/i_c and Q_a/Q_c ratios are not independent of scan rate, which also indicates that the process is not electrochemically reversible. As the scan rate increases, the i_a/i_c and Q_a/Q_c ratios decrease and approach the unity value. In this case, the voltammogram appears more reversible at higher scan rates, as it is to be expected [51].

Another indication of the non-reversibility of the reactions is the values of anodic and cathodic peaks separation ($E_a - E_c$) shown in Table 2 since they are much greater than $59\ mV/n$, which is considered a threshold value for reversible reactions [51]. In this case, the irreversibility of the reactions occurring in the tested solutions follows the trend: Bi+HCl < Sb+HCl < Sb+Bi+HCl. This irreversible behavior of the electrodeposition of Sb and Bi, when they are separated or present together may be explained by the extremely high acidity of the solutions since protons act as a barrier to electron transfer making the process sluggish [50]. In any case, further studies should be conducted to shed more light on the irreversible behavior of the reactions. Considering the similarity of the behavior of the peaks at scan rates between 0.05 V/s - 0.02 V/s, the next evaluations will be carried out at 0.02 V/s.

3.3. Sb and Bi concentration

The influence of the concentration of Sb and Bi on the cyclic voltammetry curves was evaluated and the results are shown in Figure 6.

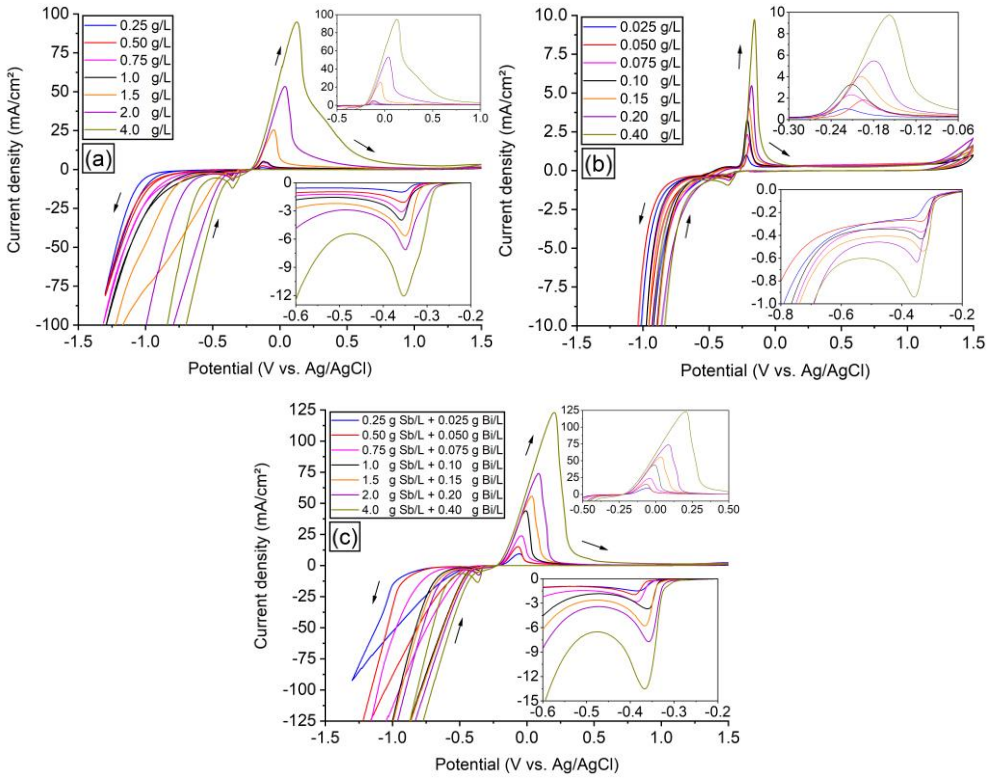

Figure 6 – Cyclic voltammograms for solutions of (a) Sb+HCl, (b) Bi+HCl and (c) Sb+Bi+HCl at different concentrations of metals (0.25 – 4.0 g/L for Sb(III) and 0.025 - 0.40 g/L for Bi(III)). Insets show the oxidation and reduction peaks.

Note that for the Sb+HCl solution (Figure 6a), the reduction peaks shift towards cathodic current densities as the concentration increases, but the potential value of the peaks remains virtually unchanged. This indicates that the antimony deposition rate is affected kinetically by its concentration. For the Bi+HCl solution (Figure 6b), the peaks showed a strong shift towards cathodic currents and a slight shift towards more negative overpotentials with increasing concentration. Therefore, the bismuth deposition rate is affected both kinetically and thermodynamically by its concentration. This difference between the electrodeposition of metals as a function of their concentration indicates a greater contribution of the migrational component to the bismuth deposition, which may be related to the difference in the diffusion controlled contribution to the mass transfer for each metal and the lower concentration of bismuth [52], as discussed in the previous sections. According to the speciation diagram (Figure S1 of Supplementary Material) constructed for each of the solutions shown in Figure 6, the increase in the concentration of Sb and Bi does not alter the type of predominant species in the solutions since their

concentrations increase practically in the same proportion. Only solutions containing Sb show an additional species ($SbCl_2^+$) when the concentration of this metal is greater than approximately 1.5 g/L.

When the potential scan is reversed, the anodic peak shows the same behavior for the three solutions: a sharp increase towards more positive currents and a subtle shift towards more positive potentials. Furthermore, Figure 6a shows that as the concentration of antimony increases in the Sb+HCl solution, the presence of a shoulder related to the dissolution of a different Sb phase becomes more prominent, which must be related to the presence of some oxide. When bismuth is present together with antimony in solution (Figure 6c), this shoulder becomes less apparent, indicating that the presence of Bi even at low concentrations may inhibit the dissolution of Sb species. The latter may explain the stronger increase in the current density of the oxidation peak shown in Figure 3 when Sb and Bi are present simultaneously in the solution.

The increase in concentration also causes an increase in the distance between the reduction and oxidation potential peaks of the metals and in the Q_a/Q_c ratios (Table S1 of Supplementary Material), especially for solutions in which antimony is present separately or together with Bi, thus indicating a more profound electrochemical irreversibility. According to Table S1, the electrochemical irreversibility is more accentuated in Sb+HCl and Sb+Bi+HCl solutions presenting Sb concentrations from 1.0 g/L - 1.5 g/L, which must be associated with the shoulder visible in the curves of the most concentrated solutions containing Sb (Figure 6). This behavior of the concentrated solutions may also be related to the formation of the $SbCl_2^+$ species, which appear in the solution only when the Sb concentration is equal to or greater than 1.5 g/L (Figure S1).

3.4. HCl concentration

The influence of HCl concentration on the cyclic voltammetry curves is shown in Figure 7.

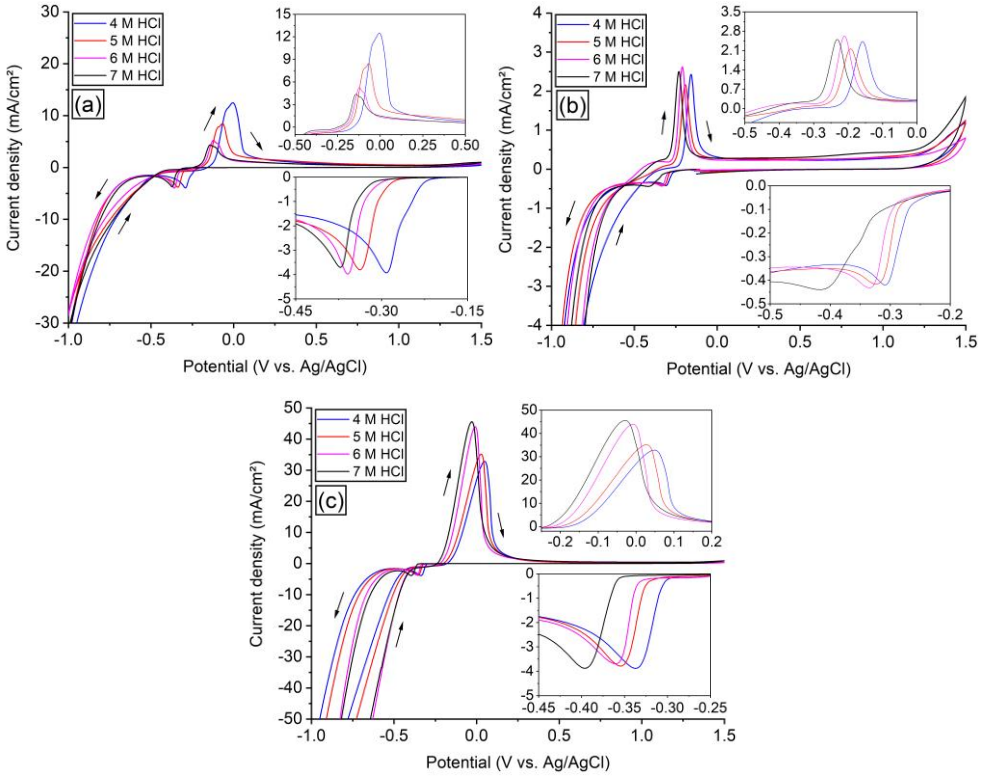

Figure 7 – Cyclic voltammograms for solutions of (a) Sb+HCl, (b) Bi+HCl and (c) Sb+Bi+HCl at different HCl concentrations (4 M – 7 M). Insets show the oxidation and reduction peaks.

The onset of Sb and Bi reduction appears at more cathodic overpotentials as the concentration of HCl increases, while the current density of the reduction peaks remains virtually unchanged. As mentioned in Section 3.2, this negative shift of potential can be explained by the extremely high concentration of H^+ ions on the electrode surface acting as a coulombic barrier to the access of the species of Sb and Bi, which hinders their electrodeposition [53]. As shown in the speciation diagram (Figure S2 of Supplementary Material) constructed for the solutions present in Figure 7, increasing HCl concentration causes a subtle difference in the predominant species containing Sb and Bi. As the concentration of HCl increases, there is an increase in the concentration of species with charge 3 ($SbCl_6^{3-}$ and $BiCl_6^{3-}$) and a reduction in the concentration of species with charge 2 ($SbCl_5^{2-}$ and $BiCl_5^{2-}$) and 1 ($SbCl_4^-$ and $BiCl_4^-$), in addition to the neutral species $SbCl_3$. Although this difference is subtle when compared to the increase in proton concentration, this may also have influenced the shift of the overpotential at which the metals are electrodeposited. In this case, operating the membrane electrolysis with less

acidic solutions would require less energy, in addition to extend the lifespan of the membranes, which should not be exposed to extreme pH conditions [38]. However, the use of HCl concentrations lower than 5 mol/L tends to hinder the extraction of Sb and Bi from the ion-exchange resins, reducing the efficiency of the resin elution step [25].

The shift of the oxidation peaks towards less positive potentials with increasing HCl concentration indicates involvement of H^+ in the stripping process of the metals. The lower the concentration of H^+, the easier the oxidation of the deposited metals, which agrees with the reduction section of the curves and with the discussions in Section 3.2.

According to Table S2 of Supplementary Materials, increasing the HCl concentration reduces the electrochemical irreversibility of the Sb and Bi electrodeposition reaction when the metals are present separately in the solution (Sb+HCl and Bi+HCl), since the Q_a/Q_c ratio approaches the unit value. On the other hand, increasing the HCl concentration intensifies the electrochemical irreversibility of the electrodeposition of both metals when they are present simultaneously in the solution of Sb+Bi+HCl. This difference in behavior is associated with the inhibition of the dissolution of Sb and Bi from the Sb-Bi phase formed when the metals are simultaneously present in the solution, leading to a strong increase in the current density of the anodic peak, as discussed in previous sections.

3.5.Dilution factor

Considering the disadvantages of conducting the elution of the resins with HCl solutions at concentrations lower than 5 mol/L and the advantages of operating the membrane electrolysis in less acidic conditions, the effect of diluting the working solution in different proportions was evaluated. Solutions presenting 35%, 50% and 75% of the concentration of the original one (100%) were studied. In this case, the anodic H_2SO_4 solution was also diluted with the same proportion of the cathodic solution. The results of the effect of the solution dilution on the cyclic voltammetry curves are shown in Figure 8.

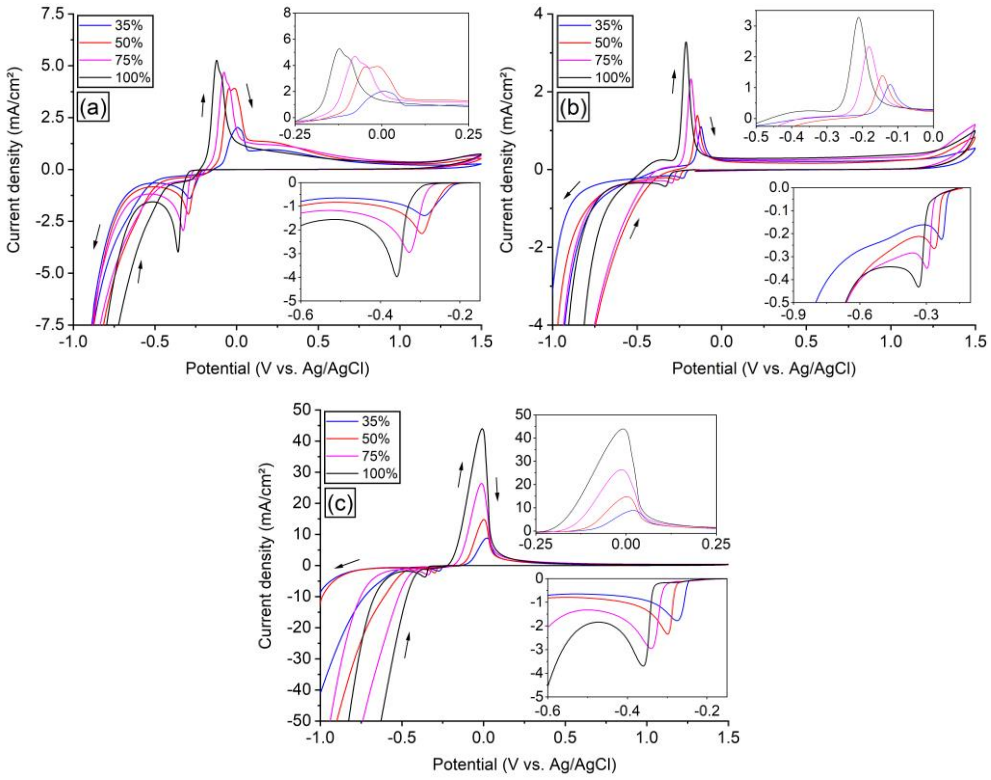

Figure 8 – Cyclic voltammograms for solutions of (a) Sb+HCl, (b) Bi+HCl and (c) Sb+Bi+HCl prepared with different dilution factors (35%, 50%, 75% and the original one – 100%). Insets show the oxidation and reduction peaks.

As can be seen, the solution dilution causes a shift of the reduction peak of the metals towards less negative potential and current densities values when the metals are separated or together in solution. This can be explained by the reduction in the conductivity of the solution as it becomes more diluted, in addition to the alteration of the predominant species present in the solution. As shown in the speciation diagrams (Figure S3 of Supplementary Material) constructed for the solutions present in Figure 8, the solution dilution favors an increase in the concentration of species with charge 1 ($SbCl_4^-$ and $BiCl_4^-$) and the neutral $SbCl_3$, while the concentration of species with charge 3 ($SbCl_6^{3-}$ and $BiCl_6^{3-}$) and 2 ($SbCl_5^{2-}$ and $BiCl_5^{2-}$) is reduced.

Regarding the oxidation of the metals in the Sb+HCl and Bi+HCl solutions, the anodic peaks show a shift towards more positive potentials and less positive current densities as the solution becomes more diluted. For the Sb+Bi+HCl solution, the oxidation peak shows a subtle change in the potential towards more positive values, while the current density becomes less positive as the dilution increases. According to Table S3, diluting

493 the solutions affects the Q_a/Q_c ratio of each of them differently. Increasing the dilution
494 of the solutions in which the metals are present separately (Sb+HCl and Bi+HCl)
495 practically does not alter the electrochemical irreversibility of the reactions. On the other
496 hand, the more the Sb+Bi+HCl solution is diluted, the more reversible the reaction
497 becomes. This difference in the behaviors supports the discussions made in sections 3.3
498 and 3.4 on the inhibition of the dissolution of Sb and Bi from the Sb-Bi phase. These
499 results suggest that diluting the working solution would decrease considerably the energy
500 consumption of the membrane electrolysis operation. On the other hand, the volume of
501 solutions to be treated would increase, and the pure HCl solution should be concentrated
502 again before returning to the elution step. One of the possible techniques that can be used
503 for this purpose is membrane distillation [54,55], but dedicated studies need to be carried
504 out to evaluate the technical and economic feasibility of the process.

505

506 3.6.Temperature

507 The effect of the temperature of the cathodic and anodic solutions on the cyclic
508 voltammetry curves was evaluated and the results are shown in Figure 9.

509

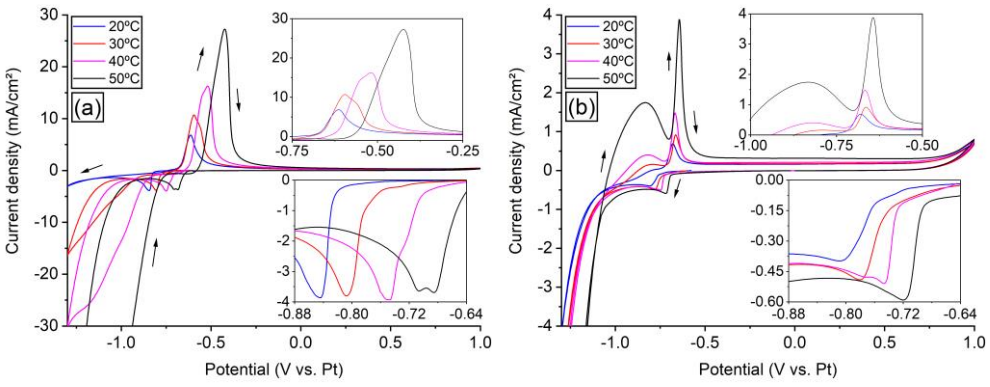

510

Figure 9 – Cyclic voltammograms for solutions of (a) Sb+HCl, (b) Bi+HCl and (c) Sb+Bi+HCl at different temperatures (20ºC, 30ºC, 40ºC and 50ºC). Insets show the oxidation and reduction peaks.

The increase in temperature between 20ºC and 50ºC showed different behaviors for the tested solutions. For Sb+HCl, the temperature increase shifts the reduction peaks towards less negative potentials, while the current density of the peaks remains practically unchanged. In this case, the greater mobility of ions in solutions at higher temperatures, which present lower viscosity and resistance, does not cause an increase in the current density of the peaks. This indicates that diffusion of Sb ions does not limit their electrodeposition, as suggested in previous sections. The curve obtained at 50ºC showed a double reduction peak, which may be related to the oxidation of Sb(III) to Sb(V) in the solution due to the high temperature followed by the reduction of both species at the electrode. Regarding the oxidation peaks during the reverse scan, the increase in temperature causes a shift towards more positive potentials, and in this case, the current density of the peaks also shows a significant increase, especially at 50ºC. According to Table S4 of Supplementary Material, increasing the temperature increases the electrochemical irreversibility of the Sb electrodeposition reaction since the area under the anodic peak increases considerably while the area under the cathodic peak remains virtually unchanged (Figure 9). For the Sb+HCl solution, it is also noted that the increase in temperature favors HER strongly, which occurs at less negative potentials when higher temperatures are used. This may reduce the current efficiency and the quality of the deposits.

For the Bi+HCl solution, the shift of the reduction peaks towards less negative potentials was accompanied by the displacement of the current density towards more negative values, differently from what was observed for the Sb+HCl solution. This difference in behavior can be attributed to the effect of temperature on the species diffusion in the solutions. As it is well-known, when the electrolyte temperature increases, the concentration of the reducible species also increases in the cathode diffusion layer due to the increase in the rates of diffusion [56]. Therefore, the increase in the concentration of Bi species at higher temperatures leads to more negative current densities, which have occurred only with bismuth because the diffusion transport control for bismuth is greater than that for antimony. When the scan is reversed, the curves of Bi+HCl solution show a

pre-wave followed by the oxidation peak, which becomes more pronounced with increasing temperature. The oxidation peaks show a shift towards more positive current densities, whereas the potential remains virtually unchanged. According to Table S4, increasing the temperature of the Bi+HCl solution increases the irreversibility of the Bi electrodeposition reaction, but in a much smaller proportion than for Sb due to the different effect of diffusion on the reduction/oxidation of each metal. The increase in temperature also favors the occurrence of HER at less positive potentials, but this effect is less pronounced for the Bi+HCl solution than for Sb+HCl one.

For the Sb+Bi+HCl solution, the behavior of the curves is very similar to that presented for Sb+HCl. Note that for 50ºC, two reduction peaks are observed due to the oxidation of Sb(III) to Sb(V) followed by the reduction of both species. The current density of the reduction peaks was practically unchanged; therefore, bismuth is not able to change this behavior of the curve, probably due to its low concentration. In all tested solutions, an increase in the current density of the anodic peak was noted with increasing temperatures. This is related to the intensification of mass transfer and the enhanced electrochemical reaction kinetics during the oxidation of the species from the electrode to the solution, which has lower resistance at higher temperatures [11]. As shown in Table S4, the increase in the current density of the anodic peaks of the Sb+HCl+HCl solution caused a strong increase in the Q_a/Q_c, ratio, indicating that the Sb-Bi phase deposition reaction becomes considerably more irreversible at higher temperatures.

The results presented in this section are in line with those recently reported by Thanu et al. [7]. The authors tested the effect of temperature on the electrolysis of Sb and Bi in hydrochloric medium by determining the amount of metals deposited on the electrode. The potential was set at -0.5V while the temperature was varied between 30ºC – 70ºC. The authors noted that increasing temperature reduces the deposition of both metals and justified this behavior by the hydrogen evolution reaction. According to our Figure 9, the potential shift towards less cathodic values with increasing temperature may have been responsible for the reduction in the electrodeposition of Sb and Bi obtained by Thanu et al. [7]. Despite this reduction in the amount of electrodeposited material observed by the authors, they noticed an increase in the cathodic current efficiency with increasing temperature, which may be related to the reduction in solution viscosity and resistance. Similar results were obtained also by Awe et al. [57] in the electrodeposition of Sb in alkaline medium.

With the current values of the reduction peaks of Sb and Bi shown in Figure 9, a graph of $\ln(i)$ vs. $1/T$ was plotted based on the Arrhenius-like expression (Equation 2) to calculate the apparent activation energy of the electrodeposition of the metals. In Equation (2), i is the peak reduction current (A), B is a constant, E_A is the apparent activation energy (kJ/mol), R is the universal gas constant (kJ/mol.K) and T is temperature (K).

$$\ln(i) = B - \frac{E_A}{RT} \qquad \text{Eq. (2)}$$

For the Sb+HCl solution, the curve of $\ln(i)$ vs. $1/T$ obtained was not linear (not shown), therefore, it was not possible to determine the apparent activation energy. For the Bi+HCl solution, the curve obtained approached a straight line (Figure 10) and the calculated E_A was 9.651 kJ/mol. This very low activation energy supports previous discussions on the diffusive control of bismuth electrodeposition [58].

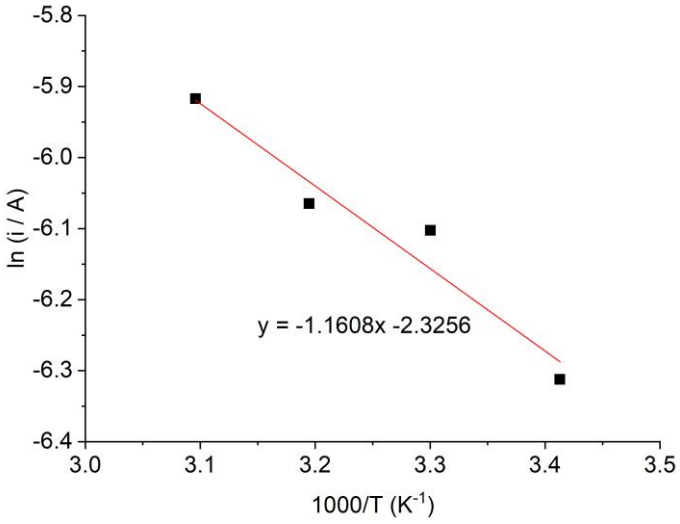

Figure 10 – Arrhenius plot for the solution of Bi+HCl.

3.7.Presence of thiourea as a complexing agent

The addition of thiourea in the elution step has been tested in recent years as it promotes the removal of Sb(V) from the ion-exchange resins, which is otherwise extremely difficult to elute with pure HCl solutions [6,25,31]. Figure 11 shows the influence of the presence of thiourea as a complexing agent on the cyclic voltammetry curves of Sb and Bi.

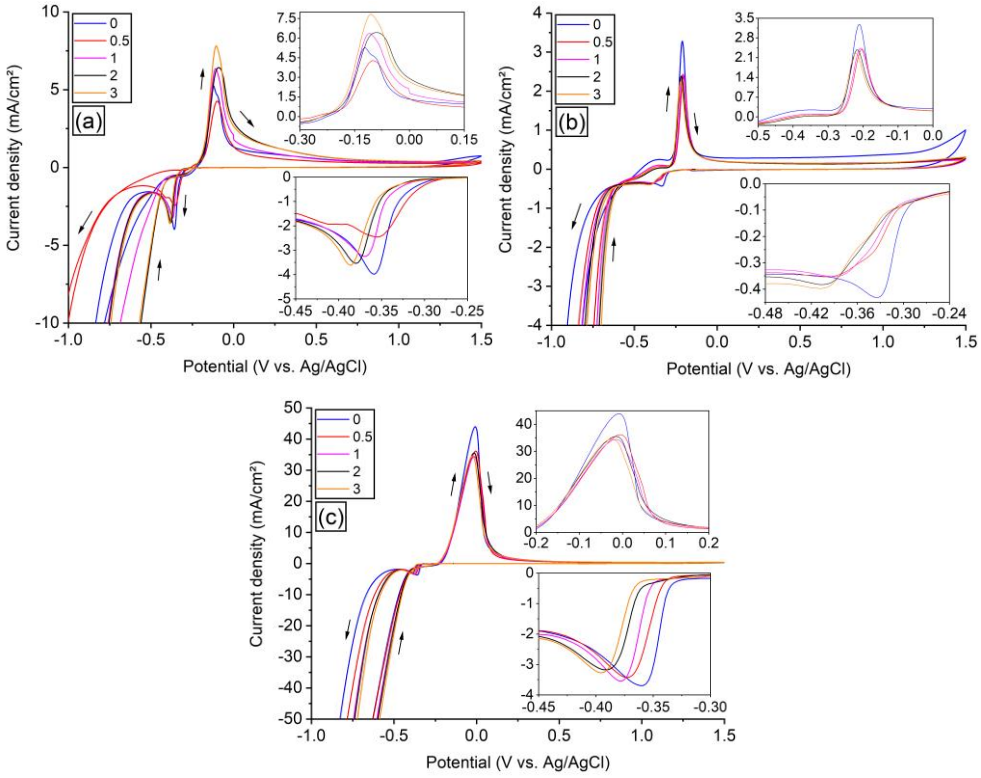

Figure 11 – Cyclic voltammograms for solutions of (a) Sb+HCl+thiourea, (b) Bi+HCl+thiourea and (c) Sb+Bi+HCl+thiourea with different thiourea/Sb molar ratios (0; 0.5; 1; 2; 3). Insets show the oxidation and reduction peaks.

Except for the curve constructed without thiourea, the behavior of the Sb+HCl (Figure 11a) and Bi+HCl (Figure 11b) solutions is very similar. In both cases, the onset of Sb and Bi reduction appears at more cathodic overpotential with the increase of thiourea concentration. The addition of thiourea causes a shift of the reduction peaks towards more negative potentials and less negative current densities. Note that for Sb+HCl solution with thiourea/Sb molar ratio of 0.5, the reduction peak splits in two, indicating that the thiourea concentration is insufficient to complex all Sb ions. For the Sb+Bi+HCl solution (Figure 11c), the addition of thiourea also causes a shift of the reduction peak towards more negative potential values, whereas the current density shows the opposite effect: a shift towards less negative values. These results suggest that the increase in thiourea concentration induces a higher inhibition of Sb and Bi reduction, which may be explained by the greater stability of Sb-thiourea and Bi-thiourea complexes: according to the Nernst equation, the increase in the stability of the metal complex causes an increase in the cathodic overpotential. Speciation diagrams for the

616 solutions shown in Figure 11 could not be constructed in the present work due to lack of
617 equilibrium constants data in the literature for reactions involving Sb-thiourea and
618 Bi-thiourea complexes in a hydrochloric medium. Another possible reason for the
619 behavior observed on the cyclic voltammogram is adsorption of thiourea on the cathode
620 surface, thus acting as a physical barrier and hindering the Sb-Bi deposition [59,60]. On
621 the other hand, the addition of thiourea may improve the homogeneity of the Sb-Bi
622 deposits as occurs in the electrodeposition of other metals [2,61]. The effects of thiourea
623 on the quality of the electrodeposits should be evaluated in further studies.

624 Regarding the oxidation peaks, they showed a reduction in current density with increasing
625 thiourea concentration, especially for the Sb+HCl and Sb+Bi+HCl solutions, which
626 supports the suggestion on the hindered deposition of the metals when thiourea is present
627 in solution [62]. According to Table S5 of Supplementary Material, increasing the
628 concentration of thiourea increases the irreversibility of the Sb electrodeposition reaction
629 in the Sb+HCl and Sb+Bi+HCl solutions, while the irreversibility for the Bi+HCl solution
630 is practically unaffected by the presence of the complexing agent. This supports the
631 previous discussions about the inhibition of the electrodeposition of the metals in the
632 presence of thiourea and the phenomenon of adsorption of thiourea on the cathode
633 surface, which occurs more intensely in solutions containing Sb.

634

635 3.8.Presence of Fe ions as an impurity

636 The influence of the presence of ferric ions was evaluated since they may also be present
637 in the electrorefining and elution solutions as an impurity [6,63]. The results obtained are
638 shown in Figure 12. The presence of iron practically does not affect the cyclic
639 voltammetry curves since the reduction and oxidation peaks remain virtually unchanged.
640 Cyclic voltammetry curves with a solution composed of Fe(III)+HCl (without Sb and Bi)
641 were also constructed to support these results and no oxidation and reduction peaks of
642 Fe(III) deposition was observed (not shown herein). Therefore, the presence of iron in the
643 solution as an impurity does not affect the deposition of Sb and Bi in the membrane
644 electrolysis. These results are supported by the speciation diagrams (Figure S4 of
645 Supplementary Material) constructed for the solutions shown in Figure 12 since the
646 addition of Fe(III) ions does not affect the composition of the complexes containing Sb
647 and Bi. Note that the main species formed containing iron are $FeCl_2^+$ and $FeCl_3$, which

do not affect the electrodeposition of the metals. This inability of iron to deposit or alter the Sb and Bi peaks is also in agreement with the literature, because iron reduction is inhibited in HCl solutions at very low pH values [64,65]. As shown in Table S6 of Supplementary Material, the presence of iron practically does not change the values of Q_a/Q_c, and therefore the irreversibility behavior of the reactions for the three solutions tested, since the reduction and oxidation peaks did not show significant changes.

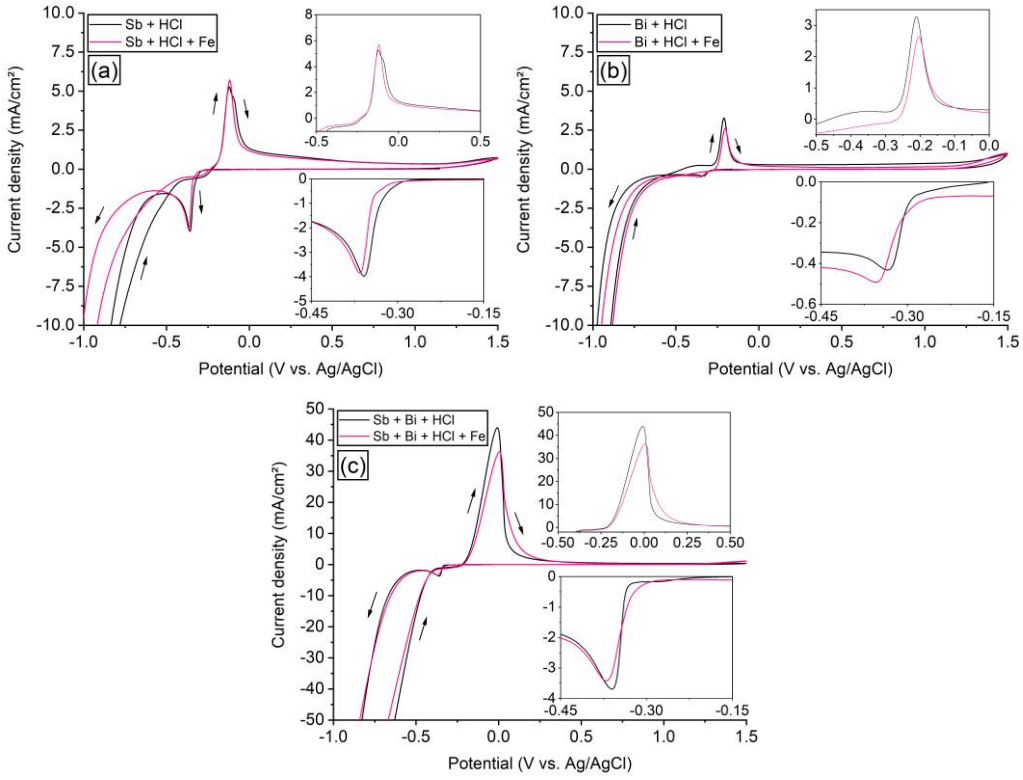

Figure 12 – Cyclic voltammograms for solutions of (a) Sb+HCl+Fe, (b) Bi+HCl+Fe and (c) Sb+Bi+HCl+Fe. Insets show the oxidation and reduction peaks.

4. Conclusions

The use of a membrane electrolysis system was proposed for recovering Sb and Bi from the elution solution of ion-exchange resins used in the treatment of copper electrorefining solutions contaminated with those metals, and a cyclic voltammetric study was carried out to evaluate the influence of the most important operating parameters on the process performance.

The results obtained showed that the reduction, and particularly the oxidation of Sb (1.0 g/L) and Bi (0.1 g/L) in HCl medium (6 mol/L), occur differently when the metals are

separated and together in solution. When they are both present, the current density needed to oxidize the metals is considerably greater than if the solution contains only one of the metals, which indicates a higher energy consumption to oxidize the phase composed of Sb-Bi.

The evaluation of the scan rate suggested that the electrodeposition reactions of both metals are not electrochemically reversible, indicating the occurrence of homogeneous kinetic or other complex phenomena taking place at the electrode. This may be associated to the extreme acidity of the tested solutions. It was also verified that the diffusion control for the bismuth electrodeposition is greater than for antimony.

The increase in Sb concentration affects its electrodeposition kinetically, whereas the increase in Bi concentration affects its electrodeposition kinetically and thermodynamically. High concentrations of HCl in the solution disfavor the electrodeposition of both metals because protons act as a coulomb barrier to the access of metals to the electrode. Although low concentrations of HCl are favorable for electrodeposition, the use of less acidic solutions in the elution step may hinder the desorption of metals. Diluting the solution before the membrane electrolysis may be an alternative, as it could reduce energy consumption.

The solution temperature had a greater effect on the electrodeposition of bismuth than antimony due to the greater control of diffusion in the electrodeposition of the former. In all cases, a lower cathodic potential is required to deposit the metals at high temperatures. On the other hand, increasing temperature favors the hydrogen evolution reaction, which may impair current efficiency. The activation energy involved in the deposition of bismuth was calculated by the Arrhenius expression and the value found was 9.651 kJ/mol.

Although the use of thiourea as a complexing agent in the elution of resins has shown to be promising for promoting the desorption of Sb(V) ions, its presence in the solution was found to impair the electrodeposition of both metals. Therefore, further studies on complexing agents capable of removing Sb(V) ions from resins and that do not hinder the recovery of Sb and Bi in membrane electrolysis should be carried out.

Lastly, the presence of iron as an impurity in the elution solution practically does not affect the electrodeposition of the metals.

Further studies should be carried out to assess in depth the irreversible behavior of the reactions shown herein, the retention/transfer of ions across the cation-exchange membrane, the influence of the ohmic drop caused by the membrane on the electrodeposition, and the quality of the deposits obtained under the range of operating conditions defined in this study.

Acknowledgments

The authors gratefully acknowledge the financial support given by the funding agencies Ministerio de Universidades de España (European Union - Next Generation EU), CNPq (Process 160320/2019-4), Cyted (Network 318RT0551), ERAMIN2 (Network Sb-RECMEMTEC, FINEP - Brazil, ANID - Chile, and Agencia Estatal de Investigación (AEI) – Spain), Dirección de Investigación Científica y Tecnológica (DICYT) of the Universidad de Santiago de Chile, UFRGS (BIC - IQR838393LRG), Agencia Estatal de Investigación (AEI) - Spain, through the project PCI2019-103535 (Co-funded by the European Regional Development Fund (FEDER), a way to build Europe). This study was financed in part by the Coordenação de Aperfeiçoamento de Pessoal de Nível Superior - Brasil (CAPES) - Finance Code 001 (Process 88887.364537/2019-00).

References

[1] J.W. Dini, D.D. Snyder, Electrodeposition of Copper, in: Mod. Electroplat., John Wiley & Sons, Inc., Hoboken, NJ, USA, 2011: pp. 33–78. doi:10.1002/9780470602638.ch2.

[2] K.S. Barros, V.S. Vielmo, B.G. Moreno, G. Riveros, G. Cifuentes, A.M. Bernardes, Chemical Composition Data of the Main Stages of Copper Production from Sulfide Minerals in Chile: A Review to Assist Circular Economy Studies, Minerals. 12 (2022). doi:10.3390/min12020250.

[3] M.E.. Schlesinger, M.J.. King, K.C.. Sole, W.G.. Davenport, Extractive Metallurgy of Copper, Elsevier, 2011. doi:10.1016/C2010-0-64841-3.

[4] G. Cifuentes, N. Guajardo, J. Hernández, Recovery of hydrochloric acid from ion

exchange processes by reactive electrodialysis, J. Chil. Chem. Soc. 60 (2015) 2711–2715. doi:10.4067/S0717-97072015000400015.

[5] X. Wang, Q. Chen, Z. Yin, M. Wang, B. Xiao, F. Zhang, Homogeneous precipitation of As, Sb and Bi impurities in copper electrolyte during electrorefining, Hydrometallurgy. 105 (2011) 355–358. doi:10.1016/j.hydromet.2010.10.004.

[6] F. Arroyo-Torralvo, A. Rodríguez-Almansa, I. Ruiz, I. González, G. Ríos, C. Fernández-Pereira, L.F. Vilches-Arenas, Optimizing operating conditions in an ion-exchange column treatment applied to the removal of Sb and Bi impurities from an electrolyte of a copper electro-refining plant, Hydrometallurgy. 171 (2017) 285–297. doi:10.1016/j.hydromet.2017.06.009.

[7] V.R.C. Thanu, M. Jayakumar, Electrochemical recovery of antimony and bismuth from spent electrolytes, Sep. Purif. Technol. 235 (2020) 116169. doi:10.1016/j.seppur.2019.116169.

[8] M. Yellishetty, D. Huston, T.E. Graedel, T.T. Werner, B.K. Reck, G.M. Mudd, Quantifying the potential for recoverable resources of gallium, germanium and antimony as companion metals in Australia, Ore Geol. Rev. 82 (2017) 148–159. doi:10.1016/j.oregeorev.2016.11.020.

[9] H. Vikström, Is There a Supply Crisis? Sweden's Critical Metals, 1917–2014, Extr. Ind. Soc. 5 (2018) 393–403. doi:10.1016/j.exis.2018.03.012.

[10] C.G. Anderson, The metallurgy of antimony, Geochemistry. 72 (2012) 3–8. doi:10.1016/j.chemer.2012.04.001.

[11] S.B. Hočevar, B. Ogorevc, J. Wang, B. Pihlar, A study on operational parameters for advanced use of bismuth film electrode in anodic stripping voltammetry, Electroanalysis. 14 (2002) 1707–1712. doi:10.1002/elan.200290014.

[12] H.U. Sverdrup, K.V. Ragnarsdottir, D. Koca, An assessment of metal supply sustainability as an input to policy: security of supply extraction rates, stocks-in-use, recycling, and risk of scarcity, J. Clean. Prod. 140 (2017) 359–372. doi:10.1016/j.jclepro.2015.06.085.

[13] S. Müller, C. Schötz, O. Picht, W. Sigle, P. Kopold, M. Rauber, I. Alber, R.

758 Neumann, M.E. Toimil-Molares, Electrochemical synthesis of Bi 1-xSb x
759 nanowires with simultaneous control on size, composition, and surface
760 roughness, Cryst. Growth Des. 12 (2012) 615–621. doi:10.1021/cg200685c.

761 [14] P.M. Vereecken, S. Ren, L. Sun, P.C. Searson, Electrodeposition of Bi[sub
762 1−x]Sb[sub x] Thin Films, J. Electrochem. Soc. 150 (2003) C131.
763 doi:10.1149/1.1545458.

764 [15] F. Besse, C. Boulanger, J.M. Lecuire, Preparation of Bi1-xSbx films by
765 electrodeposition, J. Appl. Electrochem. 30 (2000) 385–392.
766 doi:10.1023/A:1003990327662.

767 [16] T. Valkova, I. Krastev, Electrodeposition of silver-bismuth alloys from
768 thiocyanate-tartrate electrolytes investigated by cyclic voltammetry, Trans. Inst.
769 Met. Finish. 80 (2002) 21–24. doi:10.1080/00202967.2002.11871422.

770 [17] F. Xiao, J. Mao, D. Cao, X. Shen, A.A. Volinsky, The role of trivalent arsenic in
771 removal of antimony and bismuth impurities from copper electrolytes,
772 Hydrometallurgy. 125–126 (2012) 76–80. doi:10.1016/j.hydromet.2012.05.011.

773 [18] X.W. Wang, Q.Y. Chen, Z.L. Yin, M.Y. Wang, F. Tang, The role of arsenic in
774 the homogeneous precipitation of As, Sb and Bi impurities in copper electrolyte,
775 Hydrometallurgy. 108 (2011) 199–204. doi:10.1016/j.hydromet.2011.04.007.

776 [19] P. Navarro, F.J. Alguacil, Adsorption of antimony and arsenic from a copper
777 electrorefining solution onto activated carbon, Hydrometallurgy. 66 (2002) 101–
778 105. doi:10.1016/S0304-386X(02)00108-1.

779 [20] K. Salari, S. Hashemian, M.T. Baei, Sb(V) removal from copper electrorefining
780 electrolyte: Comparative study by different sorbents, Trans. Nonferrous Met.
781 Soc. China. 27 (2017) 440–449. doi:10.1016/S1003-6326(17)60050-5.

782 [21] P. Navarro, J. Simpson, F.J. Alguacil, Removal of antimony (III) from copper in
783 sulphuric acid solutions by solvent extraction with LIX 1104SM,
784 Hydrometallurgy. 53 (1999) 121–131. doi:10.1016/S0304-386X(99)00033-X.

785 [22] A. Artzer, M. Moats, J. Bender, Removal of Antimony and Bismuth from Copper
786 Electrorefining Electrolyte: Part II—An Investigation of Two Proprietary Solvent
787 Extraction Extractants, Jom. 70 (2018) 2856–2863. doi:10.1007/s11837-018-

788 3129-0.

789 [23] S.A. Awe, K. Sandström, Selective leaching of arsenic and antimony from a
790 tetrahedrite rich complex sulphide concentrate using alkaline sulphide solution,
791 Miner. Eng. 23 (2010) 1227–1236. doi:10.1016/j.mineng.2010.08.018.

792 [24] L. Cifuentes, G. Crisóstomo, J.P. Ibáñez, J.M. Casas, F. Alvarez, G. Cifuentes,
793 On the electrodialysis of aqueous H2SO4-CuSO4 electrolytes with metallic
794 impurities, J. Memb. Sci. 207 (2002) 1–16. doi:10.1016/S0376-7388(01)00733-5.

795 [25] P.A. Riveros, The removal of antimony from copper electrolytes using amino-
796 phosphonic resins: Improving the elution of pentavalent antimony,
797 Hydrometallurgy. 105 (2010) 110–114. doi:10.1016/j.hydromet.2010.08.008.

798 [26] P.A. Riveros, J.E. Dutrizac, R. Lastra, A study of the ion exchange removal of
799 antimony(III) and antimony(V) from copper electrolytes, Can. Metall. Q. 47
800 (2008) 307–316. doi:10.1179/cmq.2008.47.3.307.

801 [27] B. McKevitt, D. Dreisinger, A comparison of various ion exchange resins for the
802 removal of ferric ions from copper electrowinning electrolyte solutions Part II:
803 Electrolytes containing antimony and bismuth, Hydrometallurgy. 98 (2009) 122–
804 127. doi:10.1016/j.hydromet.2009.04.007.

805 [28] I. Ruiz, G. Rios, C. Arbizu, U. Hanschke, I. Burke, Pilot tests on bismuth and
806 antimony removal from electrolyte at atlantic copper refinery, Eur. Metall. Conf.
807 EMC 2013. (2013) 85–98.

808 [29] K. Ando, N. Tsuchida, Recovering Bi and Sb from electrolyte in copper
809 electrorefining, Jom. 49 (1997) 49–51. doi:10.1007/s11837-997-0033-4.

810 [30] F. Moghimi, A.H. Jafari, H. Yoozbashizadeh, M. Askari, Adsorption behavior of
811 Sb(III) in single and binary Sb(III)—Fe(II) systems on cationic ion exchange
812 resin: Adsorption equilibrium, kinetic and thermodynamic aspects, Trans.
813 Nonferrous Met. Soc. China. 30 (2020) 236–248. doi:10.1016/S1003-
814 6326(19)65195-2.

815 [31] P.A. Riveros, Method to remove antimony from copper electrolytes, US
816 8,349187 B2, 2009.

817 [32] K. Kryst, P. (Rocky) Simmons, Antimony and Bismuth Control in Copper

Electrolyte by Ion Exchange, in: Springer International Publishing, 2018: pp. 2107–2111. doi:10.1007/978-3-319-95022-8_176.

[33] K. Dermentzis, Removal of nickel from electroplating rinse waters using electrostatic shielding electrodialysis/electrodeionization, J. Hazard. Mater. 173 (2010) 647–652. doi:10.1016/j.jhazmat.2009.08.133.

[34] T.A. Kurniawan, G.Y.S. Chan, W.H. Lo, S. Babel, Physico-chemical treatment techniques for wastewater laden with heavy metals, Chem. Eng. J. 118 (2006) 83–98. doi:10.1016/j.cej.2006.01.015.

[35] B. Van der Bruggen, Ion-exchange membrane systems-Electrodialysis and other electromembrane processes, Elsevier Inc., 2018. doi:10.1016/B978-0-12-813483-2.00007-1.

[36] T. Scarazzato, K.S. Barros, T. Benvenuti, M.A. Siqueira Rodrigues, D.C. Romano Espinosa, A. Moura Bernardes, V. Pérez-Herranz, Achievements in electrodialysis processes for wastewater and water treatment, Elsevier Inc., 2020. doi:10.1016/B978-0-12-817378-7.00005-7.

[37] M. Paidar, V. Fateev, K. Bouzek, Membrane electrolysis—History, current status and perspective, Electrochim. Acta. 209 (2016) 737–756. doi:10.1016/j.electacta.2016.05.209.

[38] K.S. Barros, M.C. Martí-Calatayud, V. Pérez-Herranz, D.C.R. Espinosa, A three-stage chemical cleaning of ion-exchange membranes used in the treatment by electrodialysis of wastewaters generated in brass electroplating industries, Desalination. 492 (2020) 114628. doi:10.1016/j.desal.2020.114628.

[39] G.C. Feijoo, K.S. Barros, T. Scarazzato, D.C.R. Espinosa, Electrodialysis for concentrating cobalt, chromium, manganese, and magnesium from a synthetic solution based on a nickel laterite processing route, Sep. Purif. Technol. 275 (2021) 119192. doi:10.1016/j.seppur.2021.119192.

[40] K.S. Barros, M.C. Martí-Calatayud, E.M. Ortega, V. Pérez-Herranz, D.C.R. Espinosa, Chronopotentiometric study on the simultaneous transport of EDTA ionic species and hydroxyl ions through an anion-exchange membrane for electrodialysis applications, J. Electroanal. Chem. 879 (2020) 114782. doi:10.1016/j.jelechem.2020.114782.

[41] G. Cifuentes, J. Simpson, C. Zúñiga, L. Briones, A. Morales, Model and simulation of an ion exchange process for the extraction of antimony, J. Metall. Eng. 1 (2012) 75–85.

[42] I. Puigdomench, Hydra Medusa — Make Equilibrium Diagrams using Sophisticated Algorithms, (2001).

[43] G.M. De Oliveira, L.L. Barbosa, R.L. Broggi, I.A. Carlos, Voltammetric study of the influence of EDTA on the silver electrodeposition and morphological and structural characterization of silver films, J. Electroanal. Chem. 578 (2005) 151–158. doi:10.1016/j.jelechem.2004.12.033.

[44] W.S. Kang, W.C. Chou, W.J. Li, T.H. Shen, C.S. Lin, Electrodeposition of Bi2Te3-based p and n-type ternary thermoelectric compounds in chloride baths, Thin Solid Films. 660 (2018) 108–119. doi:10.1016/j.tsf.2018.06.001.

[45] K.S. Barros, E.M. Ortega, V. Pérez-Herranz, D.C.R. Espinosa, Evaluation of brass electrodeposition at RDE from cyanide-free bath using EDTA as a complexing agent, J. Electroanal. Chem. 865 (2020) 114129. doi:10.1016/j.jelechem.2020.114129.

[46] M. García-Gabaldón, J. Carrillo-Abad, E. Ortega-Navarro, V. Pérez-Herranz, Electrochemical study of a simulated spent pickling solution, Int. J. Electrochem. Sci. 6 (2011) 506–519.

[47] S. Fletcher, C.S. Halliday, D. Gates, M. Westcott, T. Lwin, G. Nelson, The response of some nucleation/growth processes to triangular scans of potential, J. Electroanal. Chem. Interfacial Electrochem. 159 (1983) 267–285. doi:10.1016/S0022-0728(83)80627-5.

[48] İ.H. Karahan, R. Özdemir, Effect of Cu concentration on the formation of Cu1−x Znx shape memory alloy thin films, Appl. Surf. Sci. 318 (2014) 100–104. doi:10.1016/j.apsusc.2014.01.119.

[49] L.R. Bard, A. J.; Faulkner, Electrochemical Methods: Fundamental and Applications, 2nd Ed., John Wiley & Sons, Inc., Hoboken, NJ, USA, 2001.

[50] N. Elgrishi, K.J. Rountree, B.D. McCarthy, E.S. Rountree, T.T. Eisenhart, J.L. Dempsey, A Practical Beginner's Guide to Cyclic Voltammetry, J. Chem. Educ.

95 (2018) 197–206. doi:10.1021/acs.jchemed.7b00361.

[51] C. Sandford, M.A. Edwards, K.J. Klunder, D.P. Hickey, M. Li, K. Barman, M.S. Sigman, H.S. White, S.D. Minteer, A synthetic chemist's guide to electroanalytical tools for studying reaction mechanisms, Chem. Sci. 10 (2019) 6404–6422. doi:10.1039/c9sc01545k.

[52] M.R.H. de. Almeida, I.A. Carlos, L.L. Barbosa, R.M. Carlos, B.S. Lima-Neto, E.M.J.A. Pallone, Voltammetric and morphological characterization of copper electrodeposition from non-cyanide electrolyte, J. Appl. Electrochem. 32 (2002) 763–773. doi:10.1023/A:1020182120035.

[53] M. Šupicová, R. Rozik, L. Trnková, R. Oriňáková, M. Gálová, Influence of boric acid on the electrochemical deposition of Ni, J. Solid State Electrochem. 10 (2006) 61–68. doi:10.1007/s10008-005-0656-8.

[54] M. Tomaszewska, M. Gryta, A.W. Morawski, Mass transfer of HCl and H2O across the hydrophobic membrane during membrane distillation, J. Memb. Sci. 166 (2000) 149–157. doi:10.1016/S0376-7388(99)00263-X.

[55] R. Liu, Y. Qin, X. Li, L. Liu, Concentrating aqueous hydrochloric acid by multiple-effect membrane distillation, Front. Chem. Sci. Eng. 6 (2012) 311–321. doi:10.1007/s11705-012-1207-3.

[56] S.M. Rashwan, Electrodeposition of Zn–Cu coatings from alkaline sulphate bath containing glycine, Trans. Inst. Met. Finish. 85 (2007) 217–224. doi:10.1179/174591907X216440.

[57] S.A. Awe, J.E. Sundkvist, N.J. Bolin, Å. Sandström, Process flowsheet development for recovering antimony from Sb-bearing copper concentrates, Miner. Eng. 49 (2013) 45–53. doi:10.1016/j.mineng.2013.04.026.

[58] S. Canegallo, V. Agrigento, C. Moraitou, A. Toussimi, L.P. Bicelli, G. Serravalle, Indium diffusion inside InBi during and after electrodeposition at various temperatures, J. Alloys Compd. 234 (1996) 211–217. doi:10.1016/0925-8388(95)02115-9.

[59] C. Ramírez, J.A. Calderón, Study of the effect of Triethanolamine as a chelating agent in the simultaneous electrodeposition of copper and zinc from non-cyanide

electrolytes, J. Electroanal. Chem. 765 (2016) 132–139. doi:10.1016/j.jelechem.2015.06.003.

[60] F.L.G. Silva, D.C.B. Do Lago, E. D'Elia, L.F. Senna, Electrodeposition of Cu-Zn alloy coatings from citrate baths containing benzotriazole and cysteine as additives, J. Appl. Electrochem. 40 (2010) 2013–2022. doi:10.1007/s10800-010-0181-z.

[61] V.C. Ho, D.T. Ngo, H.T.T. Le, R. Verma, H.S. Kim, C.N. Park, C.J. Park, Effect of an organic additive in the electrolyte on suppressing the growth of Li dendrites in Li metal-based batteries, Electrochim. Acta. 279 (2018) 213–223. doi:10.1016/j.electacta.2018.05.078.

[62] S. Fashu, C.D. Gu, J.L. Zhang, M.L. Huang, X.L. Wang, J.P. Tu, Effect of EDTA and NH4Cl additives on electrodeposition of Zn−Ni films from choline chloride-based ionic liquid, Trans. Nonferrous Met. Soc. China. 25 (2015) 2054–2064. doi:10.1016/S1003-6326(15)63815-8.

[63] T. Nagai, Purification of copper electrolyte by solvent extraction and ion-exchange techniques, Miner. Process. Extr. Metall. Rev. 17 (1997) 143–168. doi:10.1080/08827509708914145.

[64] G. Csicsovszki, T. Kékesi, T.I. Török, Selective recovery of Zn and Fe from spent pickling solutions by the combination of anion exchange and membrane electrowinning techniques, Hydrometallurgy. 77 (2005) 19–28. doi:10.1016/j.hydromet.2004.10.020.

[65] J. Carrillo-Abad, M. García-Gabaldón, V. Pérez-Herranz, Electrochemical recovery of zinc from the spent pickling solutions coming from hot dip galvanizing industries. Galvanostatic operation, Int. J. Electrochem. Sci. 7 (2012) 5442–5456. doi:10.1016/j.seppur.2011.07.029.